

ORIGINAL ARTICLE

SPECT/CT imaging of baculovirus biodistribution in rat

JK Rätty^{1,2}, T Liimatainen³, T Huhtala⁴, MU Kaikkonen^{1,2}, KJ Airene^{1,2}, JM Hakumäki^{3,5}, A Närvänen⁴ and S Ylä-Herttuala^{1,6}

¹Department of Biotechnology and Molecular Medicine, AI Virtanen Institute for Molecular Sciences, University of Kuopio, Kuopio, Finland; ²Ark Therapeutics Oy, Kuopio, Finland; ³Cellular and Molecular Imaging Group, Department of Biomedical NMR, AI Virtanen Institute for Molecular Sciences, University of Kuopio, Kuopio, Finland; ⁴Department of Chemistry, University of Kuopio, Kuopio, Finland; ⁵Department of Clinical Radiology, University of Kuopio, Kuopio, Finland and ⁶Department of Medicine and Gene Therapy Unit, University of Kuopio, Kuopio, Finland

Non-invasive imaging provides essential information regarding the biodistribution of gene therapy vectors and it can also be used for the development of targeted vectors. In this study, we have utilized micro Single-photon emission computed tomography to visualize biodistribution of a ^{99m}Tc-polylys-ser-DTPA-biotin-labelled avidin-displaying baculovirus, Baavi, after intrafemoral (i.f.), intraperitoneal (i.p.), intramuscular (i.m.) and intracerebroventricular (i.c.v.) administration. The imaging results suggest that the virus can spread via the lymphatic network after different administra-

tion routes, also showing accumulation in the nasal area after systemic administration. Extensive expression in the kidneys and spleen was seen after i.p. administration, which was confirmed by reverse transcriptase-polymerase chain reaction and immunohistochemistry. Additionally, transduction of kidneys was seen with i.m. and i.f. administrations. We conclude that baculovirus may be beneficial for the treatment of kidney diseases after i.p. administration route. Gene Therapy (2007) 14, 930–938; doi:10.1038/sj.gt.3302934; published online 5 April 2007

Keywords: baculovirus; avidin; biodistribution; SPECT; imaging

Introduction

Single-photon emission computer tomography (SPECT) has been widely utilized clinically for imaging cancer metastases¹ and preclinically for screening the biodistribution of targeted substances.² Gamma-emitting isotopes such as ^{99m}Tc, ¹¹¹In, ¹²³I, ¹²⁵I and ¹³¹I are most widely used, resulting in planar or three-dimensional (3D) images. In gene therapy imaging, particle biodistribution and transductional imaging studies have shown potential in the development of improved gene therapy vectors.³ Although the results from the transgene expression pattern are vital for the success of gene therapy, biodistribution of the viral particles needs to be carefully studied as well. For example, viral particle accumulation in organs such as liver could cause immunoresponse even if the virus was unable to express any transgene. Therefore, real-time imaging of the viral particle distribution will generate important safety information and results about the kinetics of administration and result in new target tissues.

For particle biodistribution imaging, non-invasive imaging has several benefits when compared to the

traditional immunological and histological methods. The ability to image the signal real-time together with accurate anatomical reference is crucial for understanding the kinetics of viral administration and optimizing the viral dose to target tissue. Previously, SPECT has been utilized in gene therapy by imaging the particle biodistribution of adenovirus knob domain,⁴ and by imaging of indium-labelled herpes simplex viruses.^{5,6}

The interest of baculoviruses as gene therapy vectors has increased tremendously during the last decade, reflecting increased demand to develop alternative gene therapy vectors. The inherent safety of baculoviruses deriving from insect host origin together with easy production and high transgene capacity have made baculoviruses a potential alternative for various *in vivo* approaches.^{7–9} Although numerous cell lines have been described to be susceptible to baculovirus transduction,^{10–13} there are yet only a few studies dealing with baculovirus biodistribution *in vivo*.^{7,14,15}

We have previously reported the construction of a novel avidin-displaying baculovirus (Baavi) with enhanced transduction efficiency *in vitro*¹⁶ and showed it to be suitable for viral particle biodistribution imaging using avidin–biotin labelling and magnetic resonance imaging (MRI).¹⁷ Here, we present biodistribution studies using Baavi in Wistar rats, the virus coated with ^{99m}Tc-labelled polylys-ser-DTPA-biotin peptide and imaged with a microSPECT/computed tomography (CT) device. Intrafemoral (i.f.), intramuscular (i.m.), intracerebroventricular (i.c.v.) and intraperitoneal (i.p.)

Correspondence: Professor Dr S Ylä-Herttuala, Department of Biotechnology and Molecular Medicine, AI Virtanen Institute for Molecular Sciences, University of Kuopio, PO Box 1627, Kuopio 70211, Finland.

E-mail: Seppo.Yla-Herttuala@uku.fi

Received 24 October 2006; revised 6 January 2007; accepted 21 January 2007; published online 5 April 2007

administration routes were applied to image short-term biodistribution of the viral vector *in vivo*, together with measurement of the distributed dose from the dissected organs. We were able to detect signs of lymphatic trafficking with i.m., i.p. and i.f. administration and could detect concentration of the signal to the nasal area after i.f. administration. The i.m. and i.f. administrations resulted in kidney transduction, whereas i.p. administration also resulted in transduction of spleen and lungs. Altogether, the study suggested that kidney might be a feasible target for baculovirus transduction by using i.p. administration.

Results

Labelling quality and imaging

With all chelate labellings (Figure 1), the peptide-bound fractions of ^{99m}Tc were higher than 90% as demonstrated by paper chromatography.

Intrafemoral administration

Intrafemoral administration was performed to analyse the systemic biodistribution of labelled baculovirus. The SPECT imaging during 5–60 min time was performed in two sections, head and abdomen, and region of interest (ROI) count averages were calculated. After the injection of labelled virus (Figure 2a), the activity in the bladder was seen to increase from 0.62 to 3.68 $\text{count s}^{-1} \text{MBq}^{-1}$ (values for 5 and 60 min) and in kidneys from 4.82 to 5.03 $\text{count s}^{-1} \text{MBq}^{-1}$. Also in the abdomen, the systemically injected radiolabelled chelate alone (Figure 2b) resulted in bladder from 0.81 to 1.22 and in kidneys from 1.15 to 1.34 $\text{count s}^{-1} \text{MBq}^{-1}$. Animals receiving Baavi also showed activity in lungs, liver and spleen (Figure 2a).

In head section, the planar images from animal head and neck showed increased radioactivity first in the lymphatic nodes of the neck with 0.002 $\text{count s}^{-1} \text{MBq}^{-1}$ during 15–25 min and then in the nasal area with 0.002 $\text{count s}^{-1} \text{MBq}^{-1}$ during 30–50 min (Figure 2c), whereas the chelate control had decreasing activity in the circulation without signs of accumulation of the signal (Figure 2d). The 3D SPECT and superimposed SPECT/CT images confirmed the positivity in the nasal area and lymphatic nodes (Figure 2e).

After the systemic injection, baculoviral transgene expression could be detected in liver and kidneys (Table 1).

Intraperitoneal administration

After i.p. injection of baculovirus, the planar images showed instant spreading of the injected dose across the abdominal cavity, confirming successful injection. During 5–60 min imaging time, the ROI count averages in abdominal organs were as follows: in kidneys from 0.49 to 0.32, in liver from 0.60 to 0.52 $\text{counts s}^{-1} \text{MBq}^{-1}$ and in bladder from 0.62 to 0.87 $\text{count s}^{-1} \text{MBq}^{-1}$. With radiolabelled chelate alone, the respective values in kidneys were from 1.04 to 1.18, in liver from 2.06 to 1.68 and in bladder from 27.11 to 16.70 $\text{count s}^{-1} \text{MBq}^{-1}$.

Baculoviral marker gene expression could be detected sporadically in lungs and brain (Table 1), and extensively in spleen and kidneys (Figure 3a and b). Transduction in the kidney was extensive in the capsule and outer cortex

area, within the tubular epithelial cells of the kidney. The marker gene expression could also be confirmed by reverse transcriptase-polymerase chain reaction (RT-PCR) and anti- β -galactosidase protein immunostaining (Figure 3c and d). We also observed that during the 60 min time, the mediastinal lymphatic nodes could also be occasionally imaged (Figure 4a).

Intramuscular administration

Intramuscular injections were administered to analyse the behaviour of baculovirus in a more localized environment. The injections were carefully placed to avoid major blood-vessels, which could affect the biodistribution. The virus spread to femoral area was seen by appearing spot areas with ROI count averages of 10.39 $\text{count s}^{-1} \text{MBq}^{-1}$ (Figure 4b) very quickly after the injections, whereas the radiolabelled chelate-injected controls showed the activity remaining only in the injection site (Figure 4c). There were very little changes in the activity of the areas during the observation time.

Interestingly, we could occasionally detect activity in the lymphatic nodes of head and neck in virus-injected animals with late imaging time points. The baculoviral transgene expression could be detected only in the kidney (Table 1).

Intracerebroventricular administration

Injections to cerebral lateral ventricle were administered to analyse the drainage of the injected dose from the brain. As compared to the animals injected with chelate control, the activity in brains after injection of labelled baculovirus was constantly lower after perfusion and dissection (Table 1), indicating faster removal of the labelled virus as compared to the radiochelate control. Additionally, the planar SPECT imaging showed ROI count average of 0.56 $\text{count s}^{-1} \text{MBq}^{-1}$ in kidneys (Figure 4d), seen first 65 min after the i.c.v. injections of labelled virus. Because of the small injected volume of the baculovirus, no transgene expression was studied.

Discussion

Owing to their safety and ease of production, baculoviruses have become attractive gene delivery vectors. Although the specific interactions between baculovirus surface proteins and target cellular receptors are not exactly known, there is a hypothesis of virus binding via heparate sulphate residues¹⁸ and phospholipids¹⁹ supported by a large number of baculovirus-susceptible cell lines *in vitro*.¹³ When considering the possible clinical use of baculoviruses, the transductional kinetics and suitable administration methods of baculoviruses *in vivo* have to be evaluated. Previously, it has been reported that baculovirus transduction *in vivo* is inhibited by the blood complement system,²⁰ and several approaches have been published to circumvent this problem.^{15,21,22} As an alternative approach, baculoviruses have been successfully used *in vivo* in immunoprivileged areas, such as the eye⁸ or central nervous system (CNS).^{7,23,24} However, large viral tropism together with reports on systemic escape⁷ and transportation via axons²⁵ raise a question for examining the baculovirus kinetics *in vivo* after different administration methods. Biodistribution studies

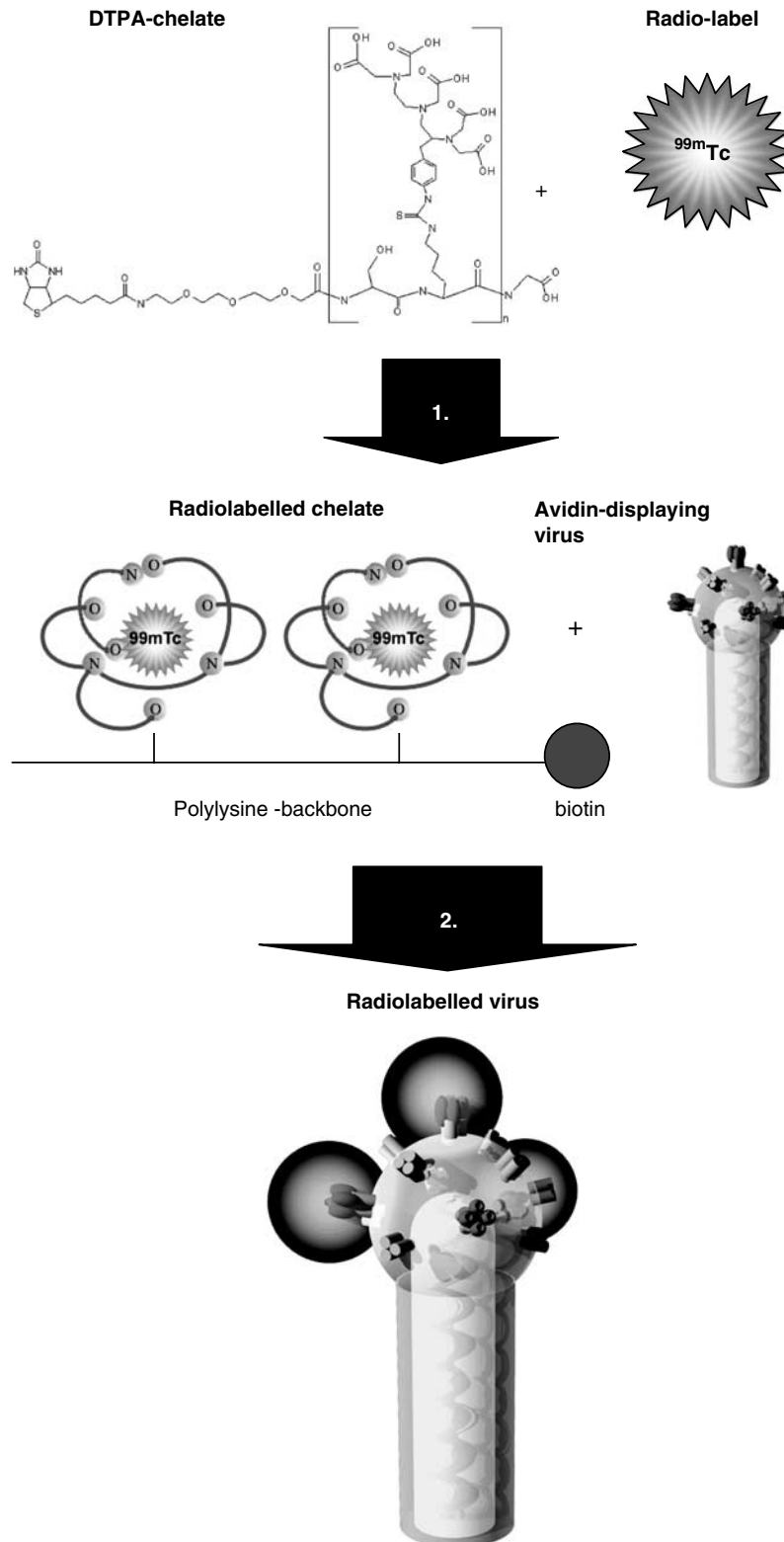


Figure 1 Labelling scheme for the avidin-displaying baculovirus with biotinylated multi lysine molecule; Biot-PEG-SKSKSKSKSKSKSKSKSKSK(Biot)-G chelate. (1) DTPA-chelate in SnCl_2 is mixed with ^{99m}Tc -pertechnetate and incubated for 10 min, resulting in radiolabelled ^{99m}Tc -poly-lys-DTPA-biotin chelate. (2) Desired volume of the radiolabelled chelate is then mixed with avidin-displaying baculovirus, resulting in radiolabelled virus.

based on the transgene expression pattern of the virus do not provide accurate information about the viral particle distribution kinetics after administration. Therefore,

tracking of viral particles can provide important information about baculovirus systemic kinetics and safety of the administration.

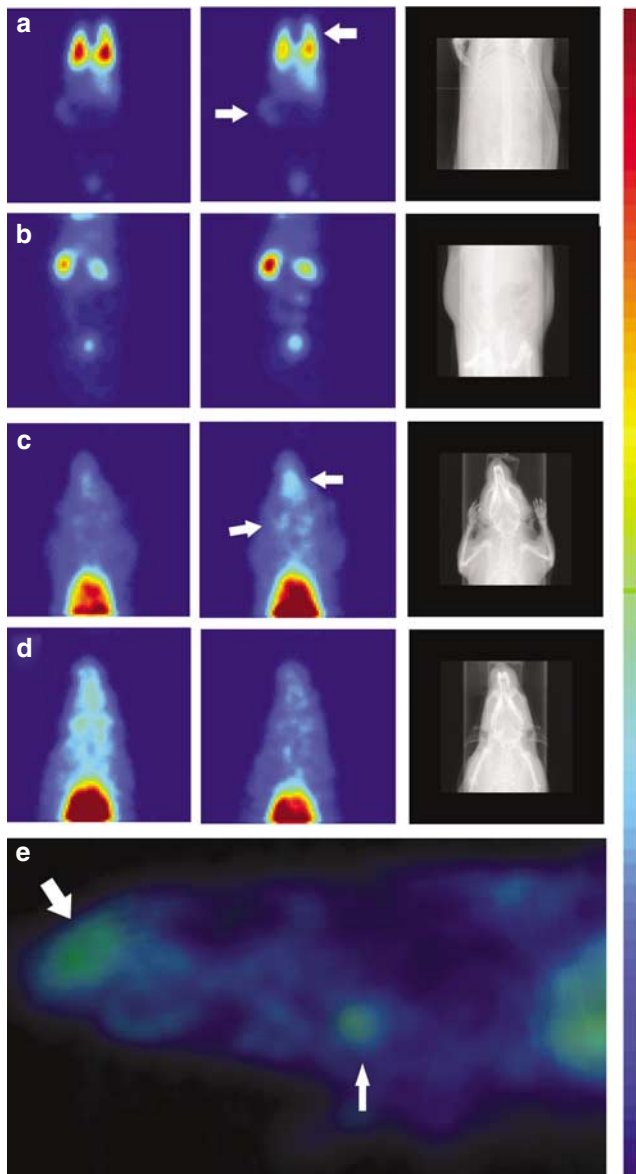


Figure 2 Planar SPECT images (at 10 and 60 min) after i.f. administration of radiolabelled Baavi or ^{99m}Tc -poly-lys-DTPA-biotin chelate alone, together with CT image (X-ray). The scale of the SPECT images is adjusted to be 0.1 maximum value in each image series (a–d). (a) Injection of radiolabelled Baavi shows activity in lungs, liver, spleen (lungs and spleen marked with arrows) and bladder, whereas (b) the control shows activity only in the kidneys, ureter and bladder. (c) Head section after Baavi injection, showing accumulation of activity (from 10 to 60 min) in the rat nasal area and lymphatics (marked with arrows), whereas the (d) control injection shows decreasing activity. (e) Sagittal 3D SPECT image of radiolabelled Baavi showing activity in the nasal area and lymphatic node (marked with arrows) in the 60 min time point.

In this study, we compared polylys-serine-DTPA chelate ^{99m}Tc -labelled baculovirus virion biodistribution by using i.f., i.m., i.c.v. and i.p. administration routes. By using a combined microSPECT/CT device, the particle biodistribution can be monitored in real time with SPECT and anatomical referencing.

To evaluate the viral behaviour with wide organ access via the circulation, we performed systemic injection via v. femoralis (i.f., Figure 2). SPECT planar imaging of viral

dose showed increasing activity in the lungs, liver, spleen and kidneys, whereas imaging of the radiolabelled chelate or ^{99m}Tc alone (data not shown) resulted in brightening of kidneys, ureters and bladder as the urinary export of water-soluble substances progressed. It has been shown that the reticulo-endothelial system of liver plays an important role in the active disposal of administered viral particles.²⁶ In agreement with this, some transgene expression could be detected in the liver, likely in macrophages (data not shown). However, contrary to i.f. injection of the wild-type virus with the labelled chelate, Baavi resulted in moderate β -galactosidase expression in kidneys and liver (Table 1). In previous studies, baculoviral gene expression could be detected in the liver, spleen and kidney after systemic tail-vein administration to complement-deficient mice.¹⁴ Another study showed green fluorescent protein (GFP) expression after i.v. administration of baculovirus in liver, spleen, lung, heart, kidney and brains of BALB/c mice,²² although no GFP or luciferase expression was seen in vesicular stomatitis virus G-protein (VSV-G) displaying baculovirus in the same strain of mice.¹⁵ The latter is interesting, as the VSV-G display has been reported to protect from the complement system of blood.²⁷ The contradiction between these two results, namely transgene expression in multiple organs or no expression, could suggest that factors other than the complement had an effect on the *in vivo* transduction of baculovirus.

Interestingly, in our study the signal after viral i.f. administration was seen to concentrate on the nasal area of the rat. Previously, feline immunodeficiency virus pseudotyped with baculovirus Gp64 glycoprotein were shown to transduce olfactory and respiratory epithelial cells²⁸ and wild-type baculovirus was shown to induce a strong innate immune response after intranasal administration,²⁹ suggesting that baculovirus might have tropism for cells in the nasal area.

When examining the radioactivity of dissected organs vs transgene expression (Table 1), the correlation was not always complete. Because baculovirus transduction contains a step for capsid transport to the nucleus, any hindrance in that step is likely to prevent marker gene expression, even while the viral tropism would result in accumulation in tissues and furthermore in a positive signal in SPECT imaging. We speculate that depending on the method of administration, the detection level for transduction might be affected by the complement and/or the poor nuclear transport within the cells, as suggested by an earlier study.³⁰

Another administration method, i.p. injection, has been used for the treatment of ovarian cancer, in an attempt to overcome the limitations of intratumoral injections for improved access to the peritoneal cavity.³¹ The i.p. injection of labelled Baavi resulted in significantly increased radioactivity in spleen and kidney detected by a gammacounter and detailed SPECT analysis. β -galactosidase stainings of spleen resulted in moderate expression of the *LacZ* transgene and strong and extensive expression in kidney (Figure 3). The results were confirmed by RT-PCR and immunohistochemistry. As spleen is known to have high concentrations of iron, we also performed control stainings without the X-gal substrate to exclude the possible reaction of ferri- and ferrocyanide to form a blue

Table 1 Distribution of the administered dose of technetium-labelled Baavi or technetium-label alone (background: backg) among the dissected organs according to the administration route

	<i>i.f.</i>			<i>i.p.</i>			<i>i.m.</i>			<i>i.c.v.</i>	
	Backg. (%)	Baavi (%)	Td	Backg. (%)	Baavi (%)	Td	Backg. (%)	Baavi (%)	Td	Backg. (%)	Baavi (%)
Brain	0.01	0.06	–	0.00	0.00	+	0.00	0.01	–	33.83 ^a	22.66
Liver	2.04	1.27	+	0.05	0.04	–	0.00	0.01	–	0.03	0.02
Kidney	2.26	4.50	+++	0.15 ^a	0.52	++++	0.03	0.05	++	0.06	0.08
Lungs	1.33	2.10	–	0.02	0.06	++	0.02	0.01	–	0.13	0.07
Heart	0.06	0.05	–	0.32	0.03	–	0.00	0.00	–	0.06	0.02
Spleen	0.05	1.60	–	0.62 ^a	6.51	+++	0.01	0.02	–	0.10	0.00
Testicle	0.06	0.16	–	0.01	0.03	–	0.00	0.02	–	0.02	0.01
Sum	0.06	0.10		0.01	7.20		0.06	0.11		34.23	22.84

Abbreviations: *i.f.*, intrafemoral; *i.p.*, intraperitoneal; *i.m.*, intramuscular; *i.c.v.*, intracerebroventricular administration.

The values are presented as percent of injected dose/gram tissue. The results from the beta-galactosidase stainings for transgene expression of labelled Baavi are shown in transduction (Td) column, in the scale of – no or extremely low transduction to ++++ very strong transduction.

^aStatistically significant difference to control with $P < 0.05$, by unpaired *t*-test.

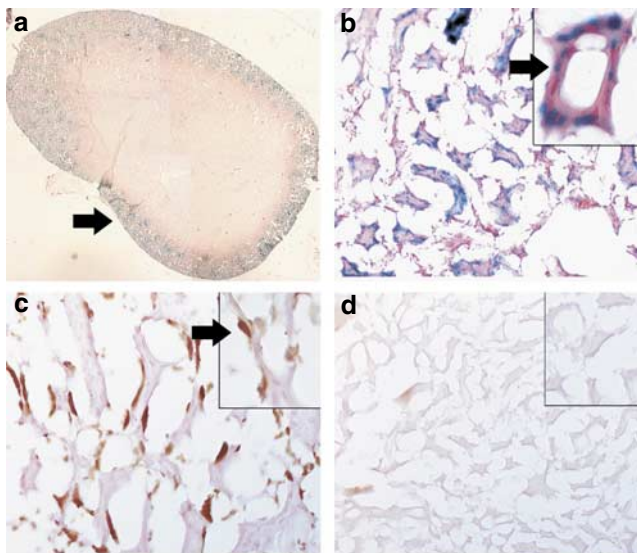


Figure 3 Rat kidney 3 days after *i.p.* injection of ^{99m}Tc-poly-lys-DTPA-biotin coated Baavi with Mayer's Carmalum counterstain. (a) Composite image of rat kidney after β -galactosidase staining, showing *LacZ* transgene expression in capsule and outer cortex area (marked with an arrow). (b) Extensive blue stain of the nuclear targeted *LacZ* transgene can be seen in tubular epithelial cells of kidney, $\times 200$ original magnification, and with more detail in the inset (marked with an arrow), $\times 400$ original magnification. (c) DAB-enhanced anti- β -galactosidase immunostaining correlates with the β -galactosidase staining for the viral transgene, $\times 200$ original magnification with detail in the inset (marked with an arrow), $\times 400$ original magnification. (d) Control staining without any virus shows no signal after anti- β -galactosidase immunohistochemistry, $\times 200$ original magnification with detail in the inset, $\times 400$ original magnification.

precipitate with free ferric iron (Prussian blue reaction). The control stainings were negative (data not shown), confirming the results.

According to the literature, baculoviruses have previously been shown to efficiently transduce various mammalian kidney cell lines *in vitro*,^{32,33} these results are also in agreement with previous results of kidney transduction *in vivo*.¹⁴ It might be possible that avidin display has enhanced the baculovirus transduction

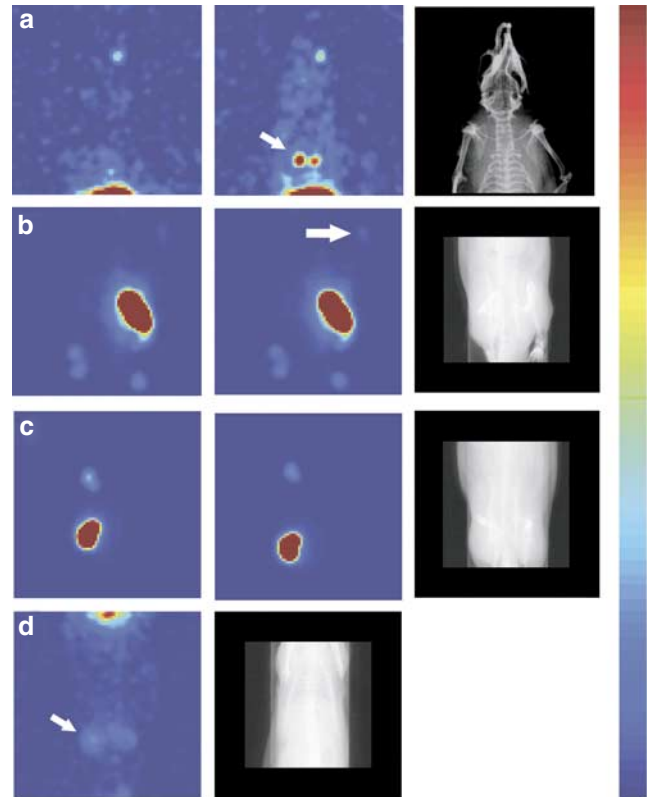


Figure 4 Planar SPECT images (10 and 60 min) with CT of Baavi or control ^{99m}Tc-poly-lys-DTPA-biotin chelate biodistribution after (b) *i.m.* injection of radiolabelled Baavi, showing escape of the activity (marked with an arrow) in comparison with (c) where chelate control shows only retention of the injected dose. (d) After *i.c.v.* injection of radiolabelled Baavi, the kidneys are seen with activity at 65 min, indicating escape from the lateral ventricle of the rat brain. (a) After *i.p.* injection of radiolabelled Baavi, the mediastinal lymphatic nodes are seen visible at the 60 min time point (marked with an arrow). The scale of the SPECT images is adjusted to be $0.1 \times$ maximum value in each image series (a–d).

mechanism, as suggested by our previous study,¹⁶ to result in efficient transduction after *i.p.* and *i.f.* administration. After *i.p.* administration, some β -galactosidase expression could also be seen in lungs and brain and

radioactivity was occasionally detected in mediastinal nodes during the SPECT imaging after i.p. administration (Figure 4a). As the peritoneal fluid enters from peritoneum to lymphatic lacunae and continues onwards via parasternal lymphatics to superior mediastinal nodes,^{34,35} our results suggest that baculovirus may enter the lymphatic circulation from the peritoneal lymphatic drainage and is able to spread systemically via lymphatics, in agreement with the results from systemic escape⁷ and distribution of avidin/biotin liposomes via lymphatic system.³⁶ Transgene expression could also be detected in the kidney cells (Table 1), indicating that injected dose might escape to systemic circulation.

Intramuscular injections have previously been successfully used in transduction of mouse skeletal muscle with VSV-G displaying baculovirus,³⁷ and in vaccination studies,^{29,38} providing data that mouse muscle might be an attractive target. Yet, in the present study, rat muscle did not result in detectable transduction, as opposed to rabbit muscle, which was transduced with VSV-GED displaying baculovirus.³⁹ It is likely that difference in the species and viral pseudotype explains this variation. However, similar to i.p. results, after i.m. Baavi injection we could detect the femoral lymphatic nodes being imaged (Figure 4b), supporting the observation of viral traffic via the lymphatic system.

When considering the transduction of cerebrospinal fluid producing *choroid plexus* cells, i.c.v. injection provides access with a limited invasion. Although CNS has been a popular target for baculovirus-mediated gene delivery, the viral kinetics after i.c.v. injection still remain obscure, providing concern about systemic escape. In this study, after i.c.v. injection of labelled Baavi or chelate alone, the remaining radioactivity in rat brain with Baavi was lower as compared to the chelate control, supporting further the theory of systemic escape. We could detect a signal in the kidneys 65 min after the i.c.v. injection (Figure 4d), indicating escape of the virus from the cerebrospinal fluid circulation, not detected with the control. As compared to the MRI,¹⁷ the lower anatomical resolution of SPECT with the small injected volume and consequent low radioactivity (5–8 MBq) prevents further pinpointing of the viral biodistribution in the brain. Interestingly, there is a report on baculoviral traffic via axons,²⁵ thus contributing to viral biodistribution with a previously unexpected manner, similarly to observation of systemic escape.⁷

When comparing different administration routes with each other, the administration via peritoneum might result in effective gene delivery to the organs in and around the abdominal cavity without strongly activating the complement system leading to virus degradation. Earlier it has been reported that the peritoneal cavity may have a diminished level of complement,⁴⁰ thus protecting the baculovirus from complement-related inactivation and favouring later transduction. This observation could also explain the stronger transduction after i.p. administration as compared to i.f. administration. We speculate that transduction from the renal capsule side could be more efficient or that during trafficking via the lymphatic system, the avidin-displaying baculovirus may become associated with lymphatic proteins/lipids, providing resistance towards complement when released back to blood circulation. It has been recently shown that peritoneal administration can be

used to reduce the side effects while reaching the therapeutics window with a smaller dose of chemotherapeutic agents.⁴¹

In conclusion, the results of this study suggest that baculoviral administration via the peritoneum might offer a new way to target kidney and treat kidney-related diseases.^{42,43} This study also suggests that baculovirus spreads via the lymphatic system and influences baculovirus transduction and biodistribution. Further studies are required to confirm traffic via the lymphatic system and the effects on gene therapy treatment and safety.

Materials and methods

Synthesis of the biotinylated multi-ser/lys molecule

Biotinylated multi-lysine molecule Biot-PEG-SKSKSKSKSKSKSKSKSKSK(Biot)-G (Figure 1) was synthesized using an Apex 396 DC multiple peptide synthesizer (Advanced ChemTech, Louisville, KY, USA) with Fmoc strategy; Fmoc-Gly-Wang (Novabiochem, Läufelfingen, Switzerland) was used as solid phase. The side-chain protecting groups used in synthesis were *t*-butyloxycarbonyl (Boc) for Lys_{1–9} or (Mtt) for Lys₁₀ and tert-butyl (tBu) for Ser. Polyethylene glycol was added to the molecule as Fmoc-protected acid (2-2-Fmoc-aminoethoxyethoxy acetic acid). After synthesis, Mtt groups were removed with 1% TFA in dichloromethane (DCM) in order to release the primary amine of Lys₁₀ on resin. Biotin was coupled to an α -amino group and a free side chain via valeriana acid TBTU/DIPEA as the coupling reagent. After cleavage, molecule was purified by HPLC (Shimadzu, Kyoto, Japan) with a C₁₈ reverse phase column (xTERRA, Waters, Milford, MA, USA) and acetonitrile (ACN) as eluent (0.1% TFA in H₂O/0–60% ACN gradient for 60 min), verified with ABI QStar LC-ESI mass spectrometer (Applied Biosystems, Foster City, CA, USA) and the purity was determined by analytical HPLC with a 240 × 1.4 mm C₁₈ column (xTERRA, Waters, Milford, MA, USA) and 0–60% ACN for 30 min. Lyophilized molecule was dissolved in water before diethylenetriaminepentaacetic acid (DTPA) labelling.

DTPA labelling

The side chains of the biotinylated multi-lys molecule were labelled with ITC-DTPA (Macrocyclics, Dallas, TX, USA) by using a molar ratio of 1:20. 10 mg of ITC-DTPA (10 mg) was suspended in 1 ml of 0.1 M sodium bicarbonate buffer (pH 9.5) and mixed with 1.73 μ mol of peptide solution (5 mg/in 300 μ l of water). The solution was mixed by end/over/end mixer overnight at room temperature. The DTPA-multi-lysine conjugate was purified with HPLC as described above and lyophilized. Lyophilized conjugate was dissolved in water (1 mg/ml) and stored at –20°C.

Radiolabelling

The DTPA-multi-lys conjugate (120 μ g) was mixed with 50 μ l fresh solution of tin(II)chloride (10 mg/ml in 10 mM HCl) in a nitrogen atmosphere. 120 μ l (120 MBq) of the ^{99m}Tc-pertechnetate elution was added and incubated at room temperature for 10 min. After incubation the radiochemical purity was tested by using instant

thin-layer chromatography (ITLC) (SG, Pall Corporation, OEM Healthcare, MI, USA) in a 13 × 1.5 cm strip and saline as the mobile phase.

Preparation of the viruses

The avidin-displaying baculovirus was constructed as described previously.¹⁶ Briefly, a β -galactosidase (*LacZ*) cassette under a cytomegalovirus (CMV) promoter was cloned into a *PvuII* site of modified pFastBac1 donor vector (Invitrogen, Carlsbad, CA, USA), resulting in a BVLacZ- plasmid. Avidin-gp64 sequence under the control of the polyhedrin promoter was subcloned into the *PstI* site of a pBACSurf-1 vector (Novagen, Madison, WI, USA). The *EcoRV/SnaBI* fragment (2173 bp) containing the avidin-gp64 cassette was then cloned between the *StuI* sites of BVLacZ, resulting in Baavi donor plasmid.

All baculoviruses were generated by using the Bac-to-Bac (Invitrogen, CA, USA) method according to the manufacturer's instructions. Purification, concentration and titration of viral particles were performed as described earlier.⁴⁴ The avidin-displaying Baavi had an end point titer of 2.5×10^{10} PFU/ml and the wild-type virus was diluted to this concentration. Injected dose was 40 μ l of virus with 300 μ g labelled peptide in a volume of 300–400 μ l with a radioactivity of 40–70 MBq, except in i.c.v. injections, where the total injected volume was 10 μ l with an injected activity of 5–8 MBq. In chelate controls, the virus volume was replaced with the same volume of PBS.

Animal studies

Male Wistar rats (0.25–0.37 kg, National Laboratory Animal Center, Kuopio, Finland) were used for the experiments. The number of animals in each group was 2–5.

Intrafemoral preparation and injections

The animals were anesthetized with 2.0% isoflurane gas anesthesia with 30:70 oxygen/nitrogen, and the femoral region was shaven and purified with ethanol. The *v. femoralis* was prepared, a canyl was prepared from an intramedic Clay Adams Brand tube (Becton Dickinson Primary Care Diagnostics, Sparks, MD, USA) and a 30-gauge needle (BD Microlance, BD, Drogheda, Ireland) was inserted.

Stereotactic injections to rat cerebral ventricles

Rats were anesthetized intraperitoneally with a solution (0.150 ml/100 g) containing fentanyl-fluanisone (Janssen-Cilag, Hypnorm, Buckinghamshire, UK) and midazolam (Roche, Dormicum, Basel, Switzerland) and placed into stereotactic apparatus (Kopf Instruments, Tujunga, CA, USA). A total volume of 10 μ l of the virus with radiolabelled chelate was injected by a Hamilton syringe and with a 27 gauge needle into the right lateral ventricle (coordinates: 1.0 mm caudal to bregma, 1.5 mm right to sutura sagittalis and into a depth of 3.5 mm).

In vivo SPECT/CT imaging

The animals were anesthetized by 1.5% isoflurane in N₂/O₂ with ratios 70:30, respectively. The animals were fixed in prone position on the bed and centre of rotation relative to gantry of the dedicated small animal SPECT/CT device (Gamma Medica, Northridge, CA, USA). Imaging was performed in two slightly overlapping

sections. For planar gamma imaging a 120–240 s acquisition time with energy window 140 keV to -10 to $+15\%$ for ^{99m}Tc and ± 10 keV for ¹¹¹In was used. 3D SPECT imaging was performed using 64 projections, 60 s/projection with matrix size 81 × 81 in 125 × 125 mm² field-of-view (FOV). CT imaging was performed using the same coordinates as SPECT with 256 projections and 1024 × 1024 projection matrix size and a voltage of 60 kV. Planar imaging was performed at the earliest possible time point after the injections (5–20 min) and alternating head to abdomen imaging at 5 min intervals. After 60 min of planar imaging, 3D SPECT was performed and the procedure was finished with CT imaging. The animals were imaged in two sections: (1) head and thorax and (2) abdomen.

Image reconstruction

SPECT 3D reconstruction was carried out using LumaGem program (Gamma Medica Northridge, CA, USA) using Butterworth sixth-order low-pass post-filtering with cutoff frequency 0.3. The same filter was used for planar gamma images. 3D CT images with dimensions of 512 × 512 × 512 matrix size in 87 × 87 × 87 mm³ FOV were obtained. Both CT and SPECT images were interpolated into final 256 × 256 × 256 size matrices by using a vendor software (Gamma Medica Inc., Northridge, CA, USA).

Activity of the organs

The radioactivity of the dissected organs was measured by a Capintec CRC-120 (Capintec, Ramsey, NJ, USA) gammacounter and the results were equalized to the initial radioactivity, organ weight and administrated total dose.

Immunohistochemistry

Animals were killed with CO₂ after the last time point and perfused with 4% PFA+7.5% sucrose via transcardiac route or by 1 × PBS for *LacZ* expression studies. After harvesting, the organs were frozen with solid carbon acid cooled isopentane (Sigma Aldrich, St Louis, MO, USA) and stored at -70°C and a sample for RT-PCR was snap-frozen with liquid nitrogen and stored at -70°C . Organs were cryosectioned and stained for β -galactosidase expression as described in Kaikkonen *et al.*³⁹ The immunostainings were performed as described previously,⁷ but anti- β -galactosidase antibody (GeneTex, San Antonio, TX, USA) was used with 1:500 dilution.

RT-PCR

RT-PCR was performed as described earlier.⁷ Briefly, the tissue sample was homogenized with a blade and Trizol (Invitrogen, Carlsbad, CA, USA). The RNA was extracted by phenol-chloroform method and cDNA was synthesized by using M-MuLV Reverse Transcriptase (Promega, Madison, WI, USA). Nested PCR was performed by using forward primers 5'-ttg gcc tag agt cga cgg and 5'-cca aga aga aac gca aag tg with respective reverse primers 5'-tga ggg gac gac gac agt at and 5'-cgc cat tcg cca ttc ag.

Statistical analysis

Prism 4 from GraphPad was used to analyse the results with analysis of variance and unpaired *t*-test to

determine whether the differences between subgroups were statistically significant.

Acknowledgements

We thank the Finnish Academy (JH and SY), the Sigrid Juselius Foundation (JH and SY), Instrumentarium Science Foundation (JH and TL), Finnish Cultural Foundation (TL), Orion Science Foundation (TL) and Ark Therapeutics Ltd (JR, MK) for support. We also thank Ms Maarit Pulkkinen, Ms Tarja Taskinen, Ms Riikka Eisto and Mr Joonas Malinen for excellent technical assistance.

References

- 1 Kersemans V, Cornelissen B, Kersemans K, Bauwens M, Dierckx RA, De SB *et al*. 123/125I-labelled 2-iodo-L-phenylalanine and 2-iodo-D-phenylalanine: comparative uptake in various tumour types and biodistribution in mice. *Eur J Nucl Med Mol Imaging* 2006; **33**: 919–927.
- 2 Meikle SR, Kench P, Kassiou M, Banati RB. Small animal SPECT and its place in the matrix of molecular imaging technologies. *Phys Med Biol* 2005; **50**: R45–R61.
- 3 Weissleder R, Mahmood U. Molecular imaging. *Radiology* 2001; **219**: 316–333.
- 4 Zinn KR, Douglas JT, Smyth CA, Liu HG, Wu Q, Krasnykh VN *et al*. Imaging and tissue biodistribution of ^{99m}Tc-labeled adenovirus knob (serotype 5). *Gene Therapy* 1998; **5**: 798–808.
- 5 Schellingerhout D, Bogdanov Jr A, Marecos E, Spear M, Breakefield X, Weissleder R. Mapping the *in vivo* distribution of herpes simplex virions. *Hum Gene Ther* 1998; **9**: 1543–1549.
- 6 Schellingerhout D, Rainov NG, Breakefield XO, Weissleder R. Quantitation of HSV mass distribution in a rodent brain tumor model. *Gene Therapy* 2000; **7**: 1648–1655.
- 7 Lehtolainen P, Tynnela K, Kannasto J, Airene KJ, Yla-Herttuala S. Baculoviruses exhibit restricted cell type specificity in rat brain: a comparison of baculovirus- and adenovirus-mediated intracerebral gene transfer *in vivo*. *Gene Therapy* 2002; **9**: 1693–1699.
- 8 Haeseleer F, Imanishi Y, Saperstein DA, Palczewski K. Gene transfer mediated by recombinant baculovirus into mouse eye. *Invest Ophthalmol Vis Sci* 2001; **42**: 3294–3300.
- 9 Wang CY, Wang S. Astrocytic expression of transgene in the rat brain mediated by baculovirus vectors containing an astrocyte-specific promoter. *Gene Therapy* 2006; **13**: 1447–1456.
- 10 Kost TA, Condreay JP. Recombinant baculoviruses as mammalian cell gene-delivery vectors. *Trends Biotechnol* 2002; **20**: 173–180.
- 11 Airene KJ, Mahonen AJ, Laitinen OH, Yla-Herttuala S. Baculovirus-mediated gene transfer: an evolving new concept. In: Templeton NS (ed). *Gene and Cell Therapy*. 2nd edn Marcel Dekker, Inc.: New York, NY, 2004, pp 181–197.
- 12 Cheng T, Xu CY, Wang YB, Chen M, Wu T, Zhang J *et al*. A rapid and efficient method to express target genes in mammalian cells by baculovirus. *World J Gastroenterol* 2004; **10**: 1612–1618.
- 13 Song SU, Shin SH, Kim SK, Choi GS, Kim WC, Lee MH *et al*. Effective transduction of osteogenic sarcoma cells by a baculovirus vector. *J Gen Virol* 2003; **84**: 697–703.
- 14 Kircheis R, Wightman L, Schreiber A, Robitza B, Rossler V, Kursal M *et al*. Polyethylenimine/DNA complexes shielded by transferrin target gene expression to tumors after systemic application. *Gene Therapy* 2001; **8**: 28–40.
- 15 Tani H, Limn CK, Yap CC, Onishi M, Nozaki M, Nishimune Y *et al*. *In vitro* and *in vivo* gene delivery by recombinant baculoviruses. *J Virol* 2003; **77**: 9799–9808.
- 16 Raty JK, Airene KJ, Marttila AT, Marjomaki V, Hytonen VP, Lehtolainen P *et al*. Enhanced gene delivery by avidin-displaying baculovirus. *Mol Ther* 2004; **9**: 282–291.
- 17 Raty JK, Liimatainen T, Wirth T, Airene KJ, Ihalainen TO, Huhtala T *et al*. Magnetic resonance imaging of viral particle biodistribution *in vivo*. *Gene Therapy* 2006; **13**: 1440–1446.
- 18 Duisit G, Saleun S, Douthe S, Barsoum J, Chadeuf G, Moullier P. Baculovirus vector requires electrostatic interactions including heparan sulfate for efficient gene transfer in mammalian cells. *J Gene Med* 1999; **1**: 93–102.
- 19 Tani H, Nishijima M, Ushijima H, Miyamura T, Matsuura Y. Characterization of cell-surface determinants important for baculovirus infection. *Virology* 2001; **279**: 343–353.
- 20 Hofmann C, Strauss M. Baculovirus-mediated gene transfer in the presence of human serum or blood facilitated by inhibition of the complement system. *Gene Therapy* 1998; **5**: 531–536.
- 21 Hofmann C, Huser A, Lehnert W, Strauss M. Protection of baculovirus-vectors against complement-mediated inactivation by recombinant soluble complement receptor type 1. *Biol Chem* 1999; **380**: 393–395.
- 22 Kim YK, Park IK, Jiang HL, Choi JY, Je YH, Jin H *et al*. Regulation of transduction efficiency by pegylation of baculovirus vector *in vitro* and *in vivo*. *J Biotechnol* 2006; **125**: 104–109.
- 23 Sarkis C, Serguera C, Petres S, Buchet D, Ridet JL, Edelman L *et al*. Efficient transduction of neural cells *in vitro* and *in vivo* by a baculovirus-derived vector. *Proc Natl Acad Sci USA* 2000; **97**: 14638–14643.
- 24 Liu X, Li K, Song J, Liang C, Wang X, Chen X. Efficient and stable gene expression in rabbit intervertebral disc cells transduced with a recombinant baculovirus vector. *Spine* 2006; **31**: 732–735.
- 25 Li Y, Wang X, Guo H, Wang S. Axonal transport of recombinant baculovirus vectors. *Mol Ther* 2004; **10**: 1121–1129.
- 26 Tao N, Gao GP, Parr M, Johnston J, Baradet T, Wilson JM *et al*. Sequestration of adenoviral vector by Kupffer cells leads to a nonlinear dose response of transduction in liver. *Mol Ther* 2001; **3**: 28–35.
- 27 Barsoum J, Brown R, McKee M, Boyce FM. Efficient transduction of mammalian cells by a recombinant baculovirus having the vesicular stomatitis virus G glycoprotein. *Hum Gene Ther* 1997; **8**: 2011–2018.
- 28 Sinn PL, Burnight ER, Hickey MA, Blissard GW, McCray Jr PB. Persistent gene expression in mouse nasal epithelia following feline immunodeficiency virus-based vector gene transfer. *J Virol* 2005; **79**: 12818–12827.
- 29 Abe T, Takahashi H, Hamazaki H, Miyano-Kurosaki N, Matsuura Y, Takaku H. Baculovirus induces an innate immune response and confers protection from lethal influenza virus infection in mice. *J Immunol* 2003; **171**: 1133–1139.
- 30 Kukkonen SP, Airene KJ, Marjomaki V, Laitinen OH, Lehtolainen P, Kankaanpaa P *et al*. Baculovirus capsid display: a novel tool for transduction imaging. *Mol Ther* 2003; **8**: 853–862.
- 31 Evans TR, Keith WN. Intra-peritoneal administration of genetic therapies: promises and pitfalls. *Minerva Ginecol* 2004; **56**: 529–538.
- 32 Liang CY, Wang HZ, Li TX, Hu ZH, Chen XW. High efficiency gene transfer into mammalian kidney cells using baculovirus vectors. *Arch Virol* 2004; **149**: 51–60.
- 33 Condreay JP, Witherspoon SM, Clay WC, Kost TA. Transient and stable gene expression in mammalian cells transduced with a recombinant baculovirus vector. *Proc Natl Acad Sci USA* 1999; **96**: 127–132.
- 34 bu-Hijleh MF, Habbal OA, Moqattash ST. The role of the diaphragm in lymphatic absorption from the peritoneal cavity. *J Anat* 1995; **186**: 453–467.

- 35 Tsilibary EC, Wissig SL. Light and electron microscope observations of the lymphatic drainage units of the peritoneal cavity of rodents. *Am J Anat* 1987; **180**: 195–207.
- 36 Medina LA, Calixto SM, Klipper R, Li Y, Phillips WT, Goins B. Mediastinal node and diaphragmatic targeting after intracavitary injection of avidin/^{99m}Tc-blue-biotin-liposome system. *J Pharm Sci* 2006; **95**: 207–224.
- 37 Pieroni L, Maione D, La Monica N. *In vivo* gene transfer in mouse skeletal muscle mediated by baculovirus vectors. *Hum Gene Ther* 2001; **12**: 871–881.
- 38 Facciabene A, Aurisicchio L, La MN. Baculovirus vectors elicit antigen-specific immune responses in mice. *J Virol* 2004; **78**: 8663–8672.
- 39 Kaikkonen MU, Rätty JK, Airene KJ, Wirth T, Heikura T, Ylä-Herttua S. Truncated vesicular stomatitis virus G protein improves baculovirus transduction efficiency *in vitro* and *in vivo*. *Gene Therapy* 2006; **13**: 304–312.
- 40 Ivanovska N, Georgieva P, Barot-Ciorbaru R. Correlation between inhibited alternative complement activity and the protective effect induced by *Nocardia lysozyme* digest (NLD) during *Klebsiella pneumoniae* infection in mice. *Int J Immunopharmacol* 1996; **18**: 515–519.
- 41 Armstrong DK, Bundy B, Wenzel L, Huang HQ, Baergen R, Lele S *et al*. Intraperitoneal cisplatin and paclitaxel in ovarian cancer. *N Engl J Med* 2006; **354**: 34–43.
- 42 Osada S, Ebihara I, Setoguchi Y, Takahashi H, Tomino Y, Koide H. Gene therapy for renal anemia in mice with polycystic kidney using an adenovirus vector encoding the human erythropoietin gene. *Kidney Int* 1999; **55**: 1234–1240.
- 43 Favre D, Ferry N, Moullier P. Critical aspects of viral vectors for gene transfer into the kidney. *J Am Soc Nephrol* 2000; **11**: S149–S153.
- 44 Airene KJ, Hiltunen MO, Turunen MP, Turunen AM, Laitinen OH, Kulomaa MS *et al*. Baculovirus-mediated periaortic gene transfer to rabbit carotid artery. *Gene Therapy* 2000; **7**: 1499–1504.